The Viscous Drag on Solids Moving Through Solids

Joe D. Goddard
Dept. of Mechanical and Aerospace Engineering, University of California, San Diego, 9500 Gilman Drive, La Jolla, CA 92093

DOI 10.1002/aic.14334
Published online January 13, 2014 in Wiley Online Library (wileyonlinelibrary.com)

An extension of the theory of Ornstein (1906) and Nye (1967) for the drag force on circular wires and other solid bodies creeping through ice by means of pressure-melting and regelation is provided. Nye's theory leads to a form of Stokes law, with rates controlled by heat conduction and lubrication flow in a thin water layer between ice and solid body. New analytical solutions are given for the corresponding drag force and torque on elliptical cylinders and spheroids for the special case of thermally thin water layers and for certain special forms of uncoupled translation and rotation that allow for single-harmonic temperature fields. The present results differ from those proposed by Nye for general body shapes in the limit of negligible thermal resistance of the water layer. Also, the present results for the drag force on elliptic cylinders do not agree with the formulae derived by Tyvand and Bejan (1992) for small ellipticity. A brief review is given for various effects that might account for certain departures of the Nye theory from experiment on circular wires, in the hope that the present results may suggest simpler experiments aimed at systematic modification of the theory to account for such anomalies. © 2014 American Institute of Chemical Engineers *AIChE J*, 60: 1488–1498, 2014
Keywords: pressure melting, ice regelation, hydrodynamic lubrication, harmonic functions, glaciers, basal melting

Introduction

The works of the brothers Thomson[1–3] and Michael Faraday[4,5] mark the beginnings of a sustained scientific fascination with "regelation," the pressure-induced thawing and refreezing of ice at solid boundaries. The Thompson theory of pressure melting has been invoked to explain phenomena as diverse as the mobility of glaciers and the reduction of sliding friction on ice skates. It is also the subject of well-known classroom experiment involving the passage of a solid wire through a block of ice, leaving scarcely a trace.*

Following a much earlier analysis of Ornstein[6] for the passage of a circular wire through ice, Nye[7]gave an insightful mathematical theory for the translational drag force on circular cylinders and certain other idealized solid bodies. According to these theories, the speed of movement is linear in the applied force and controlled by a lubrication-type flow around the body in a thin interfacial water layer, combined with conduction of heat through wire, ice, and water. Thus, one encounters an interesting generalization of the classical Stefan problem, in which the usual heat conduction is now coupled with viscous flow and pressure-induced change of melting temperature. Despite this complexity, the remarkable works of Ornstein and Nye demonstrate the existence of simple analytical solutions based on the angular symmetry of the associated harmonic temperature and pressure fields. Their work provides considerable impetus to the present study, which demonstrates that one can still obtain exact analytical solutions for bodies with more complex symmetry, provided the thermal resistance of the melt layer can be neglected.

As a cautionary note on the underlying model, we recall that numerous careful experiments, several cited by Nye,[7] show only limited agreement with theory. This state of affairs has spurred subsequent theoretical speculation and further experiment, briefly summarized here.

In conjunction with Nye's work, Frank[8] predicts an instability of the freezing front behind the wire as a possible explanation of irregular ice–water structures seen in its wake. Known more generally as "Mullins–Sekerka" instability,[9,10] it is now recognized as responsible for "mushy zones," with interesting rheology and mechanics.[11] Although such irregularity would vitiate the Nye model, it is not clear that it could explain the general reduction in speed observed in most experiments.

Drake and Shreve[12] conducted further careful experiments, also providing a critical historical survey of theory and experiment on round wires and offering various explanations for the failure of the Nye theory. Their extensive analysis of experimental data reveals a nonlinear drag at low force, with speeds much less than those predicted by the Nye theory, followed by a transition at large forces to speeds closer to theory. This anomalous behavior is generally much more pronounced for high-conductivity wires.

Prior to the transition mentioned above, Drake and Shreve[12] point up the existence of a trace or "wake" of liquid and vapor bubbles behind the wire, which they attribute to the freezing-front instability, without considering the possible cavitation in lubricating layers discussed elsewhere.[13–15] At any rate, their general conclusion is that, depending on the thermal conductivity of the wires, the departures from Nye's

Correspondence concerning this article should be addressed to J. D. Goddard at jgoddard@ucsd.edu.

*See, for example, http://serc.carleton.edu/sp/compadre/demonstrations/examples/pressure_melt.html.

theory are mainly due to freezing-point depression by impurities dissolved in the ice, or by supercooling associated with finite rates of freezing, as suggested earlier by Nye. The elementary mathematical analysis of these effects by Drake and Shreve[12] leads one to hope that simple modifications of Nye's theory may be sufficient to explain discrepancies with experiment.

To finish this cursory review, some mention should be made of some other possible implications of microscopically thin water layers, such as frictional melting and "premelting." As suggested by the experiments of Evans et al.,[16] tribological effects arising from surface roughness, solid friction, and energy dissipation could affect the above regelation experiments, although they are doubtless much more important in high-speed processes such as ice skating.[17] Also, we recall the possible existence of microscopic "premelted" water layers on solid ice,[18–20] anticipated by Faraday[5] as part of his critique the Thomson theory of pressure-melting, and now believed to involve Van-der-Waals "disjoining forces."[20] Recent numerical simulations[21] indicate that hydrophobic surface forces act to retard the motion of nanowires through ice. Although such effects should be much less important for larger bodies, one cannot rule out a well-known breakdown of lubricating films at low velocities with transition to the so-called "boundary-lubrication" regime involving virtual solid–solid contact.[22] Moreover, the inevitable lateral drainage in the typical moving-wire experiment could also lead to greatly reduced melt-layer thickness at low speeds.

Setting aside complications arising from the above effects, the following analysis aims to systematize the theory of Nye and to derive analytical solutions for various body shapes undergoing rotation as well as translation. Although the set of analytical solutions is limited, the present formulation could facilitate the numerical solution of more complex body shapes and motions, and it may also suggest alternative experimental configurations for the study of regelation.

It should be noted that a previous work on the translation of slightly elliptical cylinders[23] already suggests the possible importance of variable melt-film thickness on lubrication pressure and melting temperature. This is borne out by the present analysis for arbitrary ellipticity, which provides a somewhat different result for the limit of small ellipticity.

The following analysis will also treat the rotation of elliptical cylinders and ellipsoids in a stationary body of ice, which leads to a doubling of the number of high and low pressure zones and a corresponding doubling of melting and regelation zones. One can anticipate further spatial multiplicity in the case of more complex bodies such as serrated cylinders, as the analog of Nye's[15] wavy-surface model of glacial sliding over rough terrain. Although we shall not consider it here, a small-amplitude approximation like that of Nye[15,23] could no doubt be used to treat the combined translation and rotation of any slightly deformed cylinder or sphere.

A major goal of the present work is to reformulate the Ornstein–Nye model in a general form that should be comprehensible to workers in the field of transport phenomena. Not only does this serve to reveal the underlying regimes and approximations in terms of relevant nondimensional parameters, but it also provides a starting point for numerical simulations that are unconstrained by certain approximations used in the present work. Furthermore, the improved formulation of the problem could facilitate the systematic analysis of effects not included in the model, such as freezing front instability and cavitation in the melt layer, which are treated in a somewhat *ad hoc* fashion by previous workers. With this in mind, the exact solutions presented below for thermally thin melt layers may be viewed as points of reference for more comprehensive models.

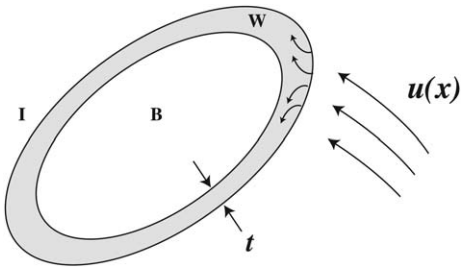

Figure 1. Schematic illustration of rigid ice mass I moving relative to rigid body B.

Mathematical Model and Analysis

As a prelude to the analysis to follow, we recall the key features of Nye's[7] model of regelation, in which a rigid thermally conductive body B undergoes a creeping motion within a stationery unbounded body of ice I, also regarded as a rigid heat conductor. Temperature and velocity fields are assumed time-independent in a frame moving with the body, as illustrated schematically in Figure 1, where the ice has velocity

$$\mathbf{u}(\mathbf{x})=\boldsymbol{\alpha}+\boldsymbol{\omega}\times\mathbf{x} \tag{1}$$

where $\boldsymbol{\alpha},\boldsymbol{\omega}$ are constant vectors representing translation and rotation of I relative to B, respectively. The relative motion (1) is accommodated by melting, regelation, and flow in a thin water film W separating B from I. Following Nye, we neglect the effects of shear stress, anisotropy of ice, and a freezing-front instability discussed below.

According to the analysis of Nye,[7†] the variation in melting temperature T_M is induced by a lubrication-type pressure variation in the water layer, with

$$T_M-T_0=-\gamma(p-p_0)\sim\gamma\mu\frac{12a^2\rho_I}{\delta^3\rho_W}U \tag{2}$$

where T_0 is the melting temperature at ambient pressure p_0, δ is a characteristic layer thickness, a an characteristic dimension of the solid body, U a characteristic relative velocity between solid body and ice, ρ_A the density of body "A," μ water viscosity, and γ the pressure-melting coefficient. The factor of 12 has been included in (2) for later notational convenience.

With the balance of heat between melting and regelation zones governed by conduction, we have

$$k\frac{(T_M-T_0)}{a}\sim\lambda\rho_I U \tag{3}$$

where λ is the specific heat of fusion of ice (energy per unit mass) and k a characteristic thermal conductivity, one obtains as characteristic length ratio or Nye number

$$\mathbb{N}=\frac{a}{\delta}=\left(\frac{a^2\rho_W\lambda}{12\mu\gamma k}\right)^{1/3}=\left\{\frac{\rho_I(a\rho_W\lambda)^2}{12\mu(\rho_W-\rho_I)kT_0}\right\}^{1/3} \tag{4}$$

†Nye uses thermal resistivity, the inverse of the thermal conductivity used here, and a volumetric latent heat given by $\rho_I\lambda$ in the present notation.

With T denoting absolute temperature, the last expression follows from the formula for γ given by linearization of the Clapeyron equation

$$\frac{d}{dp}\ln T_{\mathrm{M}} = -\frac{(\rho_{\mathrm{W}}-\rho_{\mathrm{I}})}{\rho_{\mathrm{I}}\rho_{\mathrm{W}}\lambda} \tag{5}$$

and it represents a more detailed form than given by Nye.[7]

With values representative of water at 0°C and with $a \approx 1\mathrm{mm}$, (4) gives $\mathbb{N} \approx 10^3$ and, hence, $\delta \approx 1\mu\mathrm{m}$. In the following, we take $k = k_{\mathrm{B}}$ in the definition (4), but even for larger values of k representative of metals such as copper our estimate of $\mathbb{N}$ is decreased at most by a factor of 10. Therefore, the water layer may generally be considered geometrically thin, in contrast to the exaggerated scale shown in Figure 1.

In addition to its hydraulic role, the layer constitutes a thermal resistance in series with the resistance presented by body B[7] and with relative magnitudes

$$\epsilon := \frac{k_{\mathrm{B}}\delta}{k_{\mathrm{W}}a} \equiv \frac{k_{\mathrm{B}}}{\mathbb{N}k_{\mathrm{W}}} \sim \frac{k_{\mathrm{B}}}{\mathbb{N}k_{\mathrm{I}}} \tag{6}$$

This represents relative thermal resistance or characteristic "thermal thickness" of the water layer, which obviously can become large for $k_{\mathrm{B}} \gg k_{\mathrm{W}}$.

As indicated by Ref. 7, the characteristic force f on the body B is determined by hydrodynamic lubrication pressures, yielding a highly magnified Stokes-law drag

$$f \sim \mathbb{N}^3 \mu U a \tag{7}$$

With the above parameter values, this gives velocities U of a few mm/h for forces $f \approx 1\mathrm{N}$. Such velocities result in exceedingly small thermal Péclet numbers, essentially the same for the water layer as for the external ice flow, and represent Nye's criterion for neglect of convective heat transfer. Moreover, the shear stress arising from shearing of the water layer engenders forces that are $O(\mathbb{N}^{-1})$ times that in (7) and hence negligible for large $\mathbb{N}$, as also recognized by Nye.

Basic equations and parameters

Following,[7] we treat the water layer as a geometrically and hydraulically thin region W lying adjacent to ∂B and having a thermal conductance k_{W}/t in a direction normal to W and a hydraulic conductance in a direction tangent to W given by hydrodynamic-lubrication theory. Then, with constant properties in B, W, I, the governing equations for the temperature field $\Theta = T - T_0$ and the lubrication pressure $P = p - p_0$ become

$$\nabla^2\Theta(\mathbf{x}) = 0, \quad \mathbf{x} \in \mathrm{B,I}, \text{ with } \Theta \to 0 \quad \text{for } |\mathbf{x}| \to \infty \tag{8}$$

$$\begin{aligned} -k_{\mathrm{I}}\frac{\partial\Theta}{\partial n}(\mathbf{x}+) - \rho_{\mathrm{I}}\lambda U_n(\mathbf{x}) &= -k_{\mathrm{B}}\frac{\partial\Theta}{\partial n}(\mathbf{x}-) \\ = \frac{k_{\mathrm{W}}}{t}[\Theta(\mathbf{x}-) - \Theta(\mathbf{x}+)], \Theta(\mathbf{x}+) &= -\gamma P(\mathbf{x}), \quad \mathbf{x} \in \mathrm{W} \end{aligned} \tag{9}$$

$$\nabla_{\mathrm{W}} \cdot \left(\frac{t^3}{12\mu}\nabla_{\mathrm{W}}P(\mathbf{x})\right) = \frac{1}{2}\nabla_{\mathrm{W}} \cdot (t\ \mathbf{u}_{\mathrm{W}}) + \frac{\rho_I}{\rho_{\mathrm{W}}}U_n(\mathbf{x}), \quad \mathbf{x} \in \mathrm{W} \tag{10}$$

where

$$U_n(\mathbf{x}) = \mathbf{u}\cdot\mathbf{n}, \frac{\partial}{\partial n} = \mathbf{n}\cdot\nabla, \mathbf{u}_{\mathrm{W}}(\mathbf{x}) = \mathbf{u} - U_n\mathbf{n}, \nabla_{\mathrm{W}} = \nabla - \mathbf{n}\frac{\partial}{\partial n} \tag{11}$$

$\mathbf{u}$ is given by (1), $\mathbf{x}\pm$ denote limiting values as $\mathbf{x} \to \mathrm{W}\pm$, representing the outside and inside of W, respectively, and $\mathbf{n}$ denotes the unit outer normal to B. Subscripts W denote projections onto W, and the lubrication Eq. 10 is standard.[22]

The set (8)–(10) represents the aforementioned generalization of the classical Stefan problem[10] involving the coupling of a Neumann problem in B to a Robin problem in I. These equations suffice presumably to determine $\Theta(\mathbf{x}), P(\mathbf{x})$, and $t(\mathbf{x})$ given $\mathbf{u}(\mathbf{x})$. The first equation of the thermal balance (9) and the right-hand side of the mass balance (10) show that melting, regelation, and water flow can be regarded as kinematically controlled through the specification of U_n. Accordingly, the resultant vector force and torque on B

$$\mathbf{f} = -\int_{\mathrm{W}} P\mathbf{n}dA, \quad \boldsymbol{\tau} = -\int_{\mathrm{W}} P\mathbf{n}\times\mathbf{x}dA \tag{12}$$

are determined by the orientation of B and the motion (1). As discussed below, Nye's solution for the translation of circular cylinders or spheres yields a constant film thickness t given by the positive root of a quartic polynomial.

Based on characteristic velocity U and body dimension a, we introduce nondimensional quantities

$$\begin{aligned} &\hat{\mathbf{x}} = \frac{\mathbf{x}}{a}, \quad \hat{\nabla} = a\nabla, \quad \hat{\mathbf{u}} = \frac{\mathbf{u}}{U}, \quad \hat{t} = \frac{t}{\delta}, \quad \hat{k}_{\mathrm{I}} = \frac{k_{\mathrm{I}}}{k_{\mathrm{B}}}, \quad \hat{k}_{\mathrm{W}} = \frac{k_{\mathrm{W}}}{k_{\mathrm{B}}}, \\ &\hat{\Theta} = \frac{k_{\mathrm{B}}\Theta}{a\rho_{\mathrm{I}}\lambda U}, \quad \hat{\Theta}_{\mathrm{M}} = -\frac{k_{\mathrm{B}}\gamma P}{a\rho_{\mathrm{I}}\lambda U}, \quad \hat{\mathbf{f}} = \frac{\mathbf{f}}{6\pi\mu a U}, \quad \hat{\boldsymbol{\tau}} = \frac{\boldsymbol{\tau}}{6\pi\mu a^2 U} \end{aligned} \tag{13}$$

where δ is given by (4) with $k = k_{\mathrm{B}}$, and the force and torque have been normalized by Stokes-law force on a sphere of radius a. Thus, (8)–(12) take on the form

$$\nabla^2\Theta(\mathbf{x}) = 0, \quad \mathbf{x} \in \mathrm{B,I}, \text{ with } \Theta \to 0 \quad \text{for } |\mathbf{x}| \to \infty \tag{14}$$

$$\begin{aligned} -k_I\frac{\partial\Theta}{\partial n}(\mathbf{x}+) - U_n(\mathbf{x}) &= -\frac{\partial\Theta}{\partial n}(\mathbf{x}-) \\ = \frac{1}{\epsilon t}[\Theta(\mathbf{x}-) - \Theta(\mathbf{x}+)], \ \Theta(\mathbf{x}+) &= \Theta_{\mathrm{M}}(\mathbf{x}), \ \mathbf{x} \in \mathrm{W} \end{aligned} \tag{15}$$

$$\nabla_{\mathrm{W}} \cdot [t^3\nabla_{\mathrm{W}}\Theta_{\mathrm{M}}(\mathbf{x})] = -U_n(\mathbf{x}), \quad \mathbf{x} \in \mathrm{W} \tag{16}$$

$$\mathbf{f} = \frac{2\mathbb{N}^3}{\pi}\int_{\mathrm{W}} \Theta_{\mathrm{M}}\mathbf{n}dA, \quad \boldsymbol{\tau} = \frac{2\mathbb{N}^3}{\pi}\int_{\mathrm{W}} \Theta_{\mathrm{M}}\mathbf{n}\times\mathbf{x}dA \tag{17}$$

where carets have now been dropped, with (11) remaining unaltered in form. In the case of an infinite cylinder moving normal to its axis, the area element dA is to be interpreted as circumferential arc length, so that (17) gives force and torque per unit length of cylinder.

On the right-hand sides of the equations given in (16) and (17), as in the following analysis, terms in

$$\frac{\rho_{\mathrm{W}}-\rho_{\mathrm{I}}}{\rho_{\mathrm{W}}} \quad \text{and} \quad \mathbb{N}^{-1}\nabla_{\mathrm{W}} \cdot (t\mathbf{u}) \tag{18}$$

are neglected. The parameter ϵ is defined by (6), and all variables and gradients in (14)–(16) are provisionally $O(1)$ in magnitude. Apart from the Clapeyron equation 5, we ignore density differences between water and ice (taking Nye's factor f equal to unity).

Table 1. Nye's Parametric Regimes

(1) $\epsilon \ll 1$	(2) $\epsilon \approx 1$	(3) $\epsilon \gg 1$
(A) $k_I \ll 1$	(B) $k_I \approx 1$	(C) $k_I \gg 1$

Comments on Nye's findings

To relate to Nye,[7] we note that his regimes "(1 A),(2 A), ..., (1 B),...," are represented by pairs selected from the rows in Table 1, where the first row represents water layers ranging from the thermally thin (1) to the thermally thick (3), whereas the second represents different relative resistance of body to ice. The thermally thin water layer $\epsilon=0$ represents the main focus of the present investigation, in which we eventually replace the last two equalities in (15) by

$$\Theta(\mathbf{x}-)=\Theta(\mathbf{x}+)=\ \Theta_M(\mathbf{x}),\ \ \mathbf{x}\in W \tag{19}$$

According to Nye[7] (p. 1259), the nondimensional drag force on a translating cylinder with $\epsilon \to 0$ is given, in the present notation, by the simple form

$$f=\frac{2V}{\pi a^3}\frac{\mathbb{N}^3}{1+k_I} \tag{20}$$

where V is cylinder volume. However, if applied to general cylinders, the implied independence of body shape is at odds with the anisotropic drag law found below.

When k_I is replaced by $2k_I$ and V by $4\pi a^3/3$, (20) one obtains Nye's exact result for the force on spheres with $\epsilon \to 0$, cited below in (58). Setting $k_I = 0$ in (20) also yields Nye's proposed result for general bodies in Case (1 A), with force independent of body shape. Once again, this is at odds with the analysis of three-dimensional (3-D) bodies presented below. As will become evident, the difference between the findings of Nye and the present work can be traced to the dependence of thermal and hydraulic resistance on body shape, as represented by variations in surface-normal metrical properties.

Bulk and surface flow potentials

The following analysis rests heavily on harmonic decompositions, about which a few remarks are in order.

Regarding U_n as given by a potential flow[‡] with velocity field $\mathbf{v}$

$$\mathbf{v}=-\nabla\Psi,\quad \mathbf{x}\in I,\ \text{with}\ \ U_n=\mathbf{v}\cdot\mathbf{n}=-\frac{\partial\Psi}{\partial n},\ \text{and}$$
$$\Psi=\Theta_M,\ \ \mathbf{x}\in W \tag{21}$$

one sees that (16) is a generalization of the equations proposed to describe potential flow in the presence of highly conductive surface layers[25] (Eqs. 2.16–2.18), with t^3 representing a variable tangential conductance on W.

As it will be useful for what follows, we set down here a slight generalization of the results derived in the appendix of Miloh and Benveniste[25] for the projection of vectorial divergence from a (Euclidean) space of dimension $m > 1$ onto a subspace W of dimension $m-1$.

In terms of orthogonal curvilinear coordinates, say, x_i, with metric coefficients $h_i, i=1,\ldots,m$, we recall first that

$$\nabla\cdot\mathbf{v}=\frac{1}{\Pi_m}\sum_{i=1}^{m}\frac{\partial}{\partial x_i}\left(\frac{\Pi_m}{h_i}v_i\right),\ \text{where}\ \Pi_m=\prod_{i=1}^{m}h_i \tag{22}$$

Then, assuming that W is represented by the surface $x_m \equiv x_W = \text{constant}$, and integrating (22) across a vanishingly thin region adjacent to W, with $ds_m = h_m dx_m$ and $t=\int ds_m$, we obtain

$$\int_0^t(\nabla\cdot\mathbf{v})ds_m=[\![v_m]\!]_W+\nabla_W\cdot t\langle\mathbf{v}\rangle_W,\ \ \langle v_i\rangle_W=\frac{1}{t}\int_0^t v_i ds_m,\ \ i=1,\ldots,m-1 \tag{23}$$

where $[\![v_m]\!]_W=[\![\mathbf{v}]\!]\cdot\mathbf{n}$ denotes the normal jump across W, and where the surface divergence $\nabla_W\cdot\mathbf{w}$ of a (tangent) vector field $\mathbf{w}$ on W is given by (22), with $\{\mathbf{v},m\}$ replaced by $\{\mathbf{w},m-1\}$ and with h_i evaluated at $x_m=x_W$. Hence, the definition of $\nabla_W\cdot(\kappa\nabla_W)$ follows on replacement of w_i by $(\kappa/h_i)\partial/\partial x_i$, where κ is any scalar field on W.

Another virtue of the representation (21) is that it allows us to express (15) in the form

$$-k_I\partial_m\Theta(\mathbf{x}+)-\partial_m\Psi(\mathbf{x}+)=-\partial_m\Theta(\mathbf{x}-)=\frac{h_W}{\epsilon t}[\Theta(\mathbf{x}-)-\Theta(\mathbf{x}+)],$$
$$\Theta(\mathbf{x}+)=\Theta_M(\mathbf{x}),\ \ \mathbf{x}\in W,\ \ \text{where}\ \ \partial_m=\partial/\partial x_m,\ \ h_W=h_m(\mathbf{x}),\mathbf{x}\in W \tag{24}$$

With Nye's assumption of separability, Θ and Ψ have the form $\Theta_M(x_1,x_2)F(x_3)$, at least locally, and it is evident that one must have $t\propto h_W(x_1,x_2)$, in order that each of member of these equations involve the same function $\Theta_M(x_1,x_2)$. However, this special form for t generally does not allow for a solution Θ_M to (16) in terms of surface harmonics, as required for compatibility with (21).

In the case of a thermally thin water layer $\epsilon = 0$, (19) applies, which leads to an analytic expression for t in terms of surface-normal metric and to solutions Θ_M in terms of surface harmonics. This can be formulated generally in any dimension m by first noting that Laplace's equation for $\Psi=\Theta_M(x_1,\ldots,x_{m-1})F(x_m)$, with $F(x_W)\equiv 1$, becomes

$$\sum_{i=1}^{m-1}\frac{1}{\Pi_{m-1}}\partial_i\left(\frac{h_W\Pi_{m-1}}{h_i^2}\partial_i\Theta_W\right)+\frac{\Theta_W}{h_W f_m}\frac{d}{dx_m}\left(f_m\frac{d}{dx_m}F\right)=0,\ \text{for}\ x_m=x_W \tag{25}$$

provided $\Pi_m/(h_m^2 f_m)$ is independent of x_m, where the function $f_m=f_m(x_m)$ is the last one of the $f_i, i=1,\ldots,m$ arising from the standard separability.[26§] Hence, by choosing $t^3=t_0^3 h_W$, where t_0^3 is a suitably chosen constant, and by taking $h_W U_n=-\Theta_W dF/dx_m|_{x_m=x_W}$, we can reduce (25) to the form (16). No attempt is made here to prove that this sufficient condition is necessary. This technique, illustrated by the special cases of elliptic cylinders and spheroids considered below, may also be useful for more general body shapes.

Planar Problems

Before assuming $\epsilon = 0$, we first consider motions of cylinders in the plane, with forces and torques in (12) representing the action on unit length of the cylinder.

[‡]Then $\mathbf{v}$ represents an inviscid irrotational fluid flow at rest far from a moving rigid body[24] (Ch. V), a flow whose enthalpy flux $\varrho_l\lambda(\mathbf{v}-k_l\nabla\Theta)$ has zero divergence and the same normal component on W as the actual one $-\varrho_l\lambda(\mathbf{u}-k_l\nabla\Theta)$.

[§]cf. http://mathworld.wolfram.com/StaeckelDeterminant.html, after correction of a typographical error on the line following Eq. 1.

Circular cylinders

Referred to cylindrical polar coordinates r, ϑ, the case of a circular cylinder $r = 1$ translating in a fixed direction (x) normal to its axis is covered by (1), with

$$\boldsymbol{\omega} \equiv 0,\ \ \boldsymbol{\alpha} = \cos\vartheta \mathbf{e}_r + \sin\vartheta \mathbf{e}_\vartheta,\ \ \mathbf{n} = \mathbf{e}_r,\ \ U_n = -\cos\vartheta,\ \ \frac{\partial}{\partial n} = \partial_r|_{r=1} \tag{26}$$

where $\mathbf{e}_r, \mathbf{e}_\vartheta$ denote unit basis vectors. Then, with $\partial_x := \partial/\partial x$ for any coordinate x, we may write

$$\nabla^2 = \frac{1}{r}\partial_r(r\partial_r) + \frac{1}{r^2}\nabla^2_{\mathrm{W}},\ \ \nabla^2_{\mathrm{W}} = \partial^2_\vartheta \tag{27}$$

As shown first by Ref. 5,6[¶] and later by Ref. 7, at least one solution to (14)–(16) has $t =$ constant and the remaining independent variables given by harmonic forms $R(r)\cos\vartheta$, with $R = A$, Br, Cr^{-1}, respectively, for $\Theta_{\mathrm{M}}(\mathbf{x}), \mathbf{x} \in \mathrm{W}$, and $\Theta(\mathbf{x}), \mathbf{x} \in \mathrm{B}, \mathrm{I}$, where A, B, C are constants. Substitution into (14)–(16) leads to simultaneous equations for A, B, C, t, and thence to the quartic equation for t

$$t^3 = \frac{1}{1+\epsilon t} + k_{\mathrm{I}} \tag{28}$$

where t, k_{I} refer to the quantities distinguished by carats in (13). We recall that Ref. 7 expresses this quartic in terms of ϵt and neglects a linear term in ϵt, giving a quartic for ϵt depending on the single parameter $\epsilon^3(1+k_{\mathrm{I}})$. Nye's insightful treatment of (15) as thermal resistances B plus W in parallel with resistance I yields a straight-forward determination of the constants A, B, C in terms of t. The force $\mathbf{f}$ in (17) is given in terms of A, and the reader is referred to Ref. 7 for the details.

General cylinders

By means of complex variables

$$z = x + \imath y = re^{\imath\vartheta},\ \ \text{with}\ \ \zeta = \zeta(z) = \xi + \imath\eta = \varrho e^{\imath\varphi} \tag{29}$$

the (Riemann) circle theorem allows us to transform a sufficiently smooth boundary $r = r_{\mathrm{W}}(\vartheta)$ of a simply connected region in the z-plane into the unit circle $\varrho = 1, 0 \le \varphi < 2\pi$, in the ζ-plane, by means of a suitable conformal map $\zeta = \zeta(z)$. To transform the basic equations to the complex plane, we make use of the well-known map between (contravariant) vector components and complex numbers

$$\mathbf{u} = u_x\mathbf{e}_x + u_y\mathbf{e}_y \mapsto u = u_z(\mathbf{u}) = u_x + \imath u_y \tag{30}$$

with

$$\bar{u}v = \mathbf{u}\cdot\mathbf{v} + \imath(\mathbf{u}\times\mathbf{v})\cdot\mathbf{e}_z,\ \ \text{where}\ v = v_z(\mathbf{v}), \mathbf{e}_z = \mathbf{e}_x\times\mathbf{e}_y \tag{31}$$

and

$$\boldsymbol{\nabla} \mapsto \bar{\partial}_z = \partial_x + \imath\partial_y, \partial_z v = \boldsymbol{\nabla}\cdot\mathbf{v} + \imath(\boldsymbol{\nabla}\times\mathbf{v})\cdot\mathbf{e}_z,\ \ \text{for}\ v = v_z(\mathbf{v}) \tag{32}$$

with overbar denoting complex conjugate. If u represents a contravariant form, then $\bar{u}$ represents the covariant form, and vice versa, so that the invariance of scalar product and covariance of vector cross product is manifest in (31).

In the following $\Re$ and $\Im$ denote real and imaginary parts, respectively. With ξ, η representing orthogonal curvilinear coordinates in the z-plane, a locally orthogonal transformation of physical-space vectors is defined by

$$u_\zeta = u(u_\xi\mathbf{e}_\xi + u_\eta\mathbf{e}_\eta) = e^{\imath\sigma}u_z,\ \ \text{with}\ \sigma = \arg\zeta', \zeta' = \frac{d\zeta}{dz} = \frac{1}{z'},\quad h_\zeta = h_\xi = h_\eta = |z'| \tag{33}$$

where the quantities h are metrical coefficients. Then, the complex representation of (1) is

$$u_z = \alpha + \imath\omega z = e^{-\imath\sigma}u_\zeta,\ \ \text{where}\ \ \alpha = \alpha_z(\boldsymbol{\alpha}), \omega \equiv \omega_z := \boldsymbol{\omega}\cdot\mathbf{e}_z \tag{34}$$

with

$$\bar{u}_z n_z = \bar{u}_\zeta n_\zeta,\ \ n_\zeta = e^{\imath\varphi} = e^{\imath\sigma_{\mathrm{W}}} n_z,\ \ \sigma_{\mathrm{W}}(\varphi) = \sigma(\varphi, \varrho)|_{\varrho=1}, \tag{35}$$

where $\mathbf{n}$ denotes the unit normal to W. As below, subscript W indicates limiting values of functions on $\mathbf{x} \in \mathrm{W}$.

Furthermore, the planar Laplacian transforms according to

$$\nabla^2 := \partial^2_x + \partial^2_y = \partial_z\partial_{\bar{z}} = \overline{\zeta'}\quad \partial_{\bar{\zeta}}(\zeta'\partial_\zeta) = |\zeta'|^2\partial_{\bar{\zeta}}\partial_\zeta = \frac{1}{h^2_\zeta}(\partial^2_\xi + \partial^2_\eta)$$
$$= \frac{1}{h^2_\zeta}\left[\frac{1}{\varrho}\partial_\varrho(\varrho\partial_\varrho) + \frac{1}{\varrho^2}\partial^2_\varphi\right],\ \ \text{with}\ \ h_\varrho = h_\zeta, h_\varphi = \varrho h_\varrho \tag{36}$$

By means of (23), (15), and (16) assume the coordinate-dependent form

$$\begin{aligned} -k_{\mathrm{I}}\partial_\varrho\Theta_+ - h_{\mathrm{W}}U_n &= -k_{\mathrm{I}}\partial_\varrho\Theta_+ - \partial_\varrho\Psi_+ \\ &= -\partial_\varrho\Theta_- = \frac{h_{\mathrm{W}}}{\epsilon t}[\Theta_- - \Theta_+],\ \ \Theta_+ = \Theta_{\mathrm{M}} \end{aligned} \tag{37}$$

$$\partial_\varphi\left(\frac{t^3}{h_{\mathrm{W}}}\partial_\varphi\Theta_{\mathrm{M}}\right) = -h_{\mathrm{W}}U_n = -\partial_\varrho\Psi_+ \tag{38}$$

where

$$\Theta_{\mathrm{M}} = \Theta_{\mathrm{M}}(\varphi),\ \ t = t(\varphi),\ \ h_{\mathrm{W}} = h_{\mathrm{W}}(\varphi) = h_\zeta(\varphi, \varrho)|_{\varrho=1},\ \ \partial_\varphi = \frac{d}{d\varphi} \tag{39}$$

with subscripts $\pm$ referring to limits at $\varrho = 1\pm$, respectively. The circular cylinder discussed above has of course $\zeta \equiv z$, with $h_{\mathrm{W}} \equiv 1$. For noncircular cylinders the distortion of coordinates, with by $h_{\mathrm{W}}(\varphi) \neq 1$, rules out solutions with constant t of the type considered by Nye.

By means of (30)–(35), the nondimensional force and torque are given, respectively, by

$$f = f_x + \imath f_y = \frac{2\mathbb{N}^3}{\pi}\oint_{\mathrm{W}}\Theta_{\mathrm{M}}n_z ds = \frac{2\mathbb{N}^3}{\pi}\int_0^{2\pi}\Theta_{\mathrm{M}}e^{\imath(\varphi-\sigma_{\mathrm{W}})}h_{\mathrm{W}}d\varphi \tag{40}$$

$$\begin{aligned} \tau &= \frac{2\mathbb{N}^3}{\pi}\oint_{\mathrm{W}}\Theta_{\mathrm{M}}\Im\{\bar{n}_z z\}ds \\ &= -\frac{2\mathbb{N}^3}{\pi}\int_0^{2\pi}\Theta_{\mathrm{M}}(\varphi)\sin\{\sigma_{\mathrm{W}}(\varphi) + \vartheta_{\mathrm{W}}(\varphi) - \varphi\}r_{\mathrm{W}}h_{\mathrm{W}}d\varphi \end{aligned} \tag{41}$$

The harmonic function Θ can be expressed generally as a linear combination of $\varrho^n\cos n\varphi$ and $\varrho^n\sin n\varphi$, with $n = \mp 1, \mp 2, \ldots$ for $\varrho \gtrless 1$, respectively, whereas the periodic functions $U_n, h_{\mathrm{W}}, \Theta_{\mathrm{M}}, t$ can be expressed as trigonometric series in $\cos n\varphi$ and $\sin n\varphi$. Without pursuing the details, it is plausible that the relations (37) and (38) would suffice to determine the unknown coefficients in the trigonometric series for $\Theta, \Theta_{\mathrm{M}}, t$, given the coefficients in the series for U_n, h_{W}, as dictated by the map $\zeta(z)$ and the motion (1). Although this is worthy of further investigation, attention will be focused in the present article on analytic solutions for the limit $\epsilon = 0$.

[¶] who considers a slightly more general form involving a linear combination of r and $1/r$ in an annular water layer of arbitrary thickness.

Solutions for $\epsilon=0$

Because of the φ-dependent scale factor h_W, it is evident from (37) to (38) that there exists no solution having constant t. Conversely, when $\epsilon=0$ we can replace (37) by

$$-k_I\partial_\varrho\Theta_+ - h_W U_n = -k_I\partial_\varrho\Theta_+ - \partial_\varrho\Psi_+ = -\partial_\varrho\Theta_- \quad \text{and} \quad \Theta_- = \Theta_+ = \Theta_M \tag{42}$$

and, as anticipated above, we can obtain a simple class of analytical solutions with

$$t^3 = t_0^3 h_W(\varphi), \quad t_0 = \text{const.} \tag{43}$$

Then, given the harmonic forms $\Theta(\varrho,\varphi)=F(\varrho)\Theta_M(\varphi)$ and $\Psi=S(\varrho)\Theta_M(\varphi)$, the relations (38) and (42) can be reduced to

$$\Theta_M' + n^2\Theta_M = 0, \text{ with } \Theta_M = \frac{h_W U_n}{M}, \quad F_+ = F_- = 1 \quad \text{at } \varrho = 1,$$
$$\text{and} \quad t_0^3 = \frac{M}{n^2}, \quad \text{where} \quad M = F'_- - k_I F'_+ = (1+k_I)n \tag{44}$$

and where, as above, subscripts $\pm$ refer to limits $\varrho \to 1\pm$. The requirement that $\boldsymbol{\Theta}(\varphi)$ be periodic and, hence, that n be integral, uniquely determines t_0 once n is specified. However, it remains to specify n and h_W, and to make this more evident we consider the special case of elliptic cylinders.

Ellipses

The special case of an elliptic cylinder B having principal semiaxes $a \geq b$ is covered by

$$\hat{z} = \hat{x} + \imath\hat{y} = \frac{1}{2}\left(\hat{\zeta} + \hat{\zeta}^{-1}\right), \text{ where } \hat{z} = \frac{z}{r_0}, \quad \hat{\zeta} = \frac{\zeta}{\varrho_0} = \exp(\chi + \imath\varphi) \tag{45}$$

with

$$\frac{\hat{x}^2}{\cosh^2\chi} + \frac{\hat{y}^2}{\sinh^2\chi} = 1, \quad \frac{\hat{x}^2}{\cos^2\varphi} - \frac{\hat{y}^2}{\sin^2\varphi} = 1 \tag{46}$$

where

$$\chi = \ln\hat{\varrho}, \quad \hat{\varrho} = |\hat{\zeta}|, \quad \varrho_0^2 = (1-\beta^2)/(1+\beta^2), \quad r_0^2 = 2(1-\beta^2)/\beta^2, \quad \beta = b/a \tag{47}$$

The surface $W=\partial B$ is defined by $\varrho=1$, with $\hat{\varrho}=1/\varrho_0$, and the limit $\beta \to 1, r_0^2 \to 4\varrho_0^2 \to 0$, yields the identity map $z=\zeta$.

We recall that circles $\varrho=$constant in the ζ-plane represent a family of confocal ellipses in the z-plane, with major and minor principal semiaxes equal to $r_0|\hat{\varrho}\pm 1/\hat{\varrho}|/2$, respectively, whereas lines $\varphi=$ constant represent the biorthogonal family of confocal hyperbolae. For this system, is easy to show that

$$z_W = r_0\cos(\varphi - \imath\chi_W), \quad z'_W = r_0\imath e^{-\imath\varphi}\sin(\varphi - \imath\chi_W), \text{ where } \chi_W = -\ln\varrho_0 \tag{48}$$

$$h_W = r_0|\sin(\varphi - \imath\chi_W)|, \quad n_z = e^{\imath(\varphi-\sigma_W)} = \imath\frac{r_0}{h_W}\sin(\varphi - \imath\chi_W) \tag{49}$$

Furthermore, (40) and (41) reduce to

$$f = \frac{r_0\mathbb{N}^3}{\pi\varrho_0}\int_0^{2\pi}\Theta_M[(1-\varrho_0^2)\cos\varphi + \imath(1+\varrho_0^2)\sin\varphi]d\varphi \tag{50}$$

$$\tau = -\frac{r_0^2\mathbb{N}^3}{\pi}\int_0^{2\pi}\Theta_M\sin 2\varphi d\varphi \tag{51}$$

Considering first the case of pure translation, $\alpha_z = e^{\imath\vartheta_0}, \omega = 0$ in (34), one readily finds by means of (48), (49) that the right-hand side of (38) is given by

$$h_W U_n = \partial_\varrho\Psi_+ \equiv h_W\Re\left\{\alpha_z e^{\imath(\sigma_W-\varphi)}\right\}$$
$$= \frac{r_0}{2\varrho_0}\left[\cos(\varphi-\vartheta_0) - \varrho_0^2\cos(\varphi+\vartheta_0)\right] \tag{52}$$

Here, ϑ_0 represents the angle of translation relative to the major principal axis of the ellipse B. Hence, $n=1$, with

$$\Theta_M(\varphi) = \frac{r_0}{2\varrho_0 t_0^3}\left[\cos(\varphi-\vartheta_0) - \varrho_0^2\cos(\varphi+\vartheta_0)\right],$$
$$\Theta = \Theta_M(\varphi)\varrho^{\mp 1}, \quad \text{for} \quad \varrho \gtrless 1, \quad \text{and} \quad t_0^3 = 1 + k_I \tag{53}$$

with the latter also given by (28) with $\epsilon=0$. The relations (53) and (40) then give the nondimensional force and torque as

$$f = -\frac{r_0^2\mathbb{N}^3}{2(1+k_I)\varrho_0^2}[(1-\varrho_0^2)^2\cos\vartheta_0 + \imath(1+\varrho_0^2)^2\sin\vartheta_0]$$
$$= -\frac{2}{1+\beta^2}[\beta^2\cos\vartheta_0 + \beta^{-2}\imath\sin\vartheta_0]f_0, \quad \text{and} \quad \tau = 0 \tag{54}$$

where f_0 denotes the magnitude of the force for $\beta=1$ on a circular cylinder. The quantity $\beta^4=(b/a)^4$ represents the ratio of drag for translation parallel and perpendicular to the major principal axis, respectively. One factor b/a represents the effect of body cross-section on melt inflow, and the remaining factor $(b/a)^3$ represents lubrication force.

The strong dependence in (54) on cross-sectional form clearly differs from the formulae of Ref. 7 Eqs. 1A–1C for the case $\epsilon=0$, which appear to ignore the effect of body shape on local film thickness and, hence, on the distribution of lubrication pressures and melting temperatures on ∂B.

The effect of body shape is suggested by the previous work of Ref. 23 for slightly elliptic cylinders, with $\beta = 1-e, e \ll 1$, although they consider the modification of drag only in the direction of the minor principal axis. It is easy to see from (54) that the drag relative to the circular cylinder should be modified by factors $(1\mp 2e)$, respectively, in the directions of the major and minor principal axes, whereas Tyvand and Bejan[23] (Eq. 42) obtain a factor $(1 + 3e/2)$ for the latter.

For the case of pure rotation, $\alpha_z=0$ in (34), it follows from (48) to (49) that

$$h_W U_n \equiv -h_W\Im\{\bar{n}_z u_z\} = -\frac{\omega r_0^2}{2}\sin 2\varphi \tag{55}$$

Again, (42)–(44) give an harmonic form, distinct from (53), with $n=2$ and

$$\Theta_M(\varphi) = \frac{\omega r_0^2}{4(1+k_I)}\sin 2\varphi, \quad \Theta = \Theta_M(\varphi)\varrho^{\mp 2},$$
$$\text{for } \varrho \gtrless 1, \text{ with } \quad t_0^3 = (1+k_I)/2 \tag{56}$$

Hence, after some algebra, one finds by means of (51) and (56) that

$$\tau = -\frac{r_0^4\mathbb{N}^3}{4(1+k_I)}\omega \quad \text{and } f = 0 \tag{57}$$

We recall that r_0 and ϱ_0 in (54) and (57) are given by (47) in terms of the axis ratio β. By choosing the

characteristic velocity in (13) as $U=a\omega_z$, we may take $\omega \equiv 1$ in (55)–(57). Given the definition of r_0, we note the strong dependence of torque in (57) on eccentricity of the elliptic cylinder. Also, we note the doubly periodic form of (55) implies two melting and two regelation zones generated by local rotational pressure or tension.

When translation and rotation are combined, $h_W U_n$ is given by the linear combinations of the harmonics in (52) and (55). As one may readily verify, (42)–(44) are no longer compatible with the implied harmonic forms for Θ and Θ_M. As indicated by the following analysis, the class of harmonic solutions are even more restricted in three dimensions.

Axisymmetric Bodies in Three Dimensions

As it is doubtful that arbitrary body shapes admit solutions involving a single harmonic, we specialize immediately to axisymmetric bodies, laying out the general theory and then considering the special case of spheroids. For later reference, we recall that Nye's exact solution to (14)–(16) for spheres with arbitrary ϵ yields a constant film thickness t given by (28) with k_I replaced by $2k_I$, and a nondimensional force given in the present notation as

$$f=\frac{8\mathbb{N}^3}{3t^3},\ \text{with}\ t^3\to(1+2k_I)\ \text{for}\ \epsilon\to 0 \tag{58}$$

For more general axisymmetric bodies, we adopt the conformal map (28) considered above, and, as a variant on the notation of Hobson,[27] pp. 410 ff., we let X, Y, Z denote Cartesian coordinates, where Z represents the axis of symmetry of body B, and

$$X+\imath Y=Re^{\imath\Phi},\quad R^2=X^2+Y^2,\quad z=Z+\imath R=re^{\imath\vartheta},\quad r^2=|z|^2=R^2+Z^2 \tag{59}$$

where $x_i=R,Z,\Phi$ and $x_i=r,\theta,\Phi$ represent cylindrical and spherical polar coordinates with unit basis vectors $\mathbf{e}_i$, respectively. Then, as an extension of (31), we can represent real 3-D space vectors $\mathbf{u}$ as elements $\underline{u}$ of an abstract two-dimensional (2-D) complex vector space defined by the invertible linear transformation

$$\mathbf{u}=u_Z\mathbf{e}_Z+u_R\mathbf{e}_R+u_\Phi\mathbf{e}_\Phi\mapsto\underline{u}=\underline{u}(\mathbf{u})=\begin{bmatrix}u_z\\ \\ u_\Phi\end{bmatrix}$$

where

$$u_z=u_Z+\imath u_R,\quad u_R=|\mathbf{u}_\perp|\cos(\Phi-\Phi_u),\quad u_\Phi=-|\mathbf{u}_\perp|\sin(\Phi-\Phi_u)$$

$$|\mathbf{u}_\perp|=(u_X^2+u_Y^2)^{1/2},\quad \Phi_u=\arctan(u_Y/u_X),\quad \mathbf{u}_\perp=u_X\mathbf{e}_X+u_Y\mathbf{e}_Y$$

with

$$\underline{u}^*\underline{v}=\bar{u}_z v_z+u_\Phi v_\Phi=\mathbf{u}\cdot\mathbf{v}+\imath(\mathbf{u}\times\mathbf{v})\cdot\mathbf{e}_\Phi,\quad \text{where}\ \underline{u}^*=[\bar{u}_z,u_\Phi] \tag{60}$$

defining a scalar product given by the standard rules for matrix multiplication.

By means of the circle map $\zeta(z)$, an axisymmetric surface, $R=R_W$ (Z) or $r=r_W(\vartheta)$, can be mapped into the sphere $0\le\Phi<2\pi, 0\le\varphi<\pi, \varrho\equiv 1$. Then, with metrical coefficients for the orthogonal systems Φ,ξ,η

$$h_\Phi=R(\xi,\eta)=\Im\{z(\zeta)\},\ \ h_\zeta=h_\xi=h_\eta=|z'|=1/|\zeta'| \tag{61}$$

the Laplacian becomes[27] p. 411

$$\nabla^2=\Re\left\{\frac{1}{R}\partial_z R\partial_z+\frac{1}{R^2}\partial_\Phi^2\right\}=\frac{1}{h_\zeta^2 R}\left\{\partial_\xi(R\partial_\xi)+\partial_\eta(R\partial_\eta)\right\}+\frac{1}{R^2}\partial_\Phi^2$$
$$\equiv\frac{1}{h_\zeta^2 R}\left\{\frac{1}{\varrho}\partial_\varrho(R\varrho\partial_\varrho)+\frac{1}{\varrho^2}\partial_\varphi(R\partial_\varphi)\right\}+\frac{1}{R^2}\partial_\Phi^2 \tag{62}$$

and (16) reduces to

$$\frac{1}{R_W}\left[\partial_\Phi\left(\frac{h_W t^3}{R_W}\partial_\Phi\Theta_M\right)+\partial_\varphi\left(\frac{R_W t^3}{h_W}\partial_\varphi\Theta_M\right)\right]=-h_W U_n=-\partial_\varrho\Psi_+ \tag{63}$$

where $R_W(\varphi)=R|_{\varrho=1}\equiv h_\Phi|_{\varrho=1}$ and $h_W(\varphi)=h_\varphi|_{\varrho=1}$ as in (39), and the element of area on W is $dA=R_W h_W d\varphi d\Phi$. Hence, as a variant of (40) and (41), and in a form complementary to (60), the force and torque are now given by (40) and (41)

$$\begin{bmatrix}f_\perp\\ \\ f_Z\end{bmatrix}=\frac{2\mathbb{N}^3}{\pi}\int_{\varphi=0}^{\pi}\int_{\Phi=0}^{2\pi}\Theta_M\begin{bmatrix}e^{\imath\Phi}\sin(\varphi-\sigma_W)\\ \\ \cos(\varphi-\sigma_W)\end{bmatrix}R_W h_W d\varphi d\Phi,$$
$$\text{with}\ f_\perp=f_X+\imath f_Y \tag{64}$$

$$\tau_\perp=\tau_X+\imath\tau_Y=\frac{2\mathbb{N}^3\imath}{\pi}\int_{\varphi=0}^{\pi}\int_{\Phi=0}^{2\pi}\Theta_M e^{\imath\Phi}\sin$$
$$(\sigma_W+\vartheta_W-\varphi)r_W R_W h_W d\varphi d\Phi \tag{65}$$

As indicated in a different notation by Hobson[27] p. 411, Laplace's equation based on the first form in (62) admits separable solutions of the form

$$\Theta=F_\xi F_\eta\exp(\pm\imath m\Phi),\ \ \text{for}\ R(\xi,\eta)=\exp(G),$$
$$G=G_\xi+G_\eta, h_\zeta^2/R^2=H_\xi+H_\eta \tag{66}$$

where the subscripts, doing double duty, serve to designate distinct functions as well as their arguments. Then, with primes denoting derivatives with respect to these arguments, the functions F must satisfy the ordinary differential equations

$$F_\alpha''+G_\alpha' F_\alpha'+(\lambda_\alpha-m^2H_\alpha)F_\alpha=0 \tag{67}$$

with

$$\alpha=\xi,\eta,\lambda_\xi=-\lambda_\eta=\text{const.} \tag{68}$$

Restricted shapes

With similar notation, another class of separable solutions $\Theta=F_\varrho F_\varphi\exp(\pm\imath m\Phi)$ arises for special cross-sectional shapes

$$h_\zeta^2/R^2=H_\varrho+H_\varphi/\varrho^2,\ \text{with}\ R(\zeta)=\frac{1}{\varrho}\exp(G), G=G_\varrho+G_\varphi \tag{69}$$

The functions F_α again satisfy (67) with, in lieu of (68)

$$\alpha=\varrho,\varphi,\ \ \lambda_\varphi=-\lambda_\varrho\varrho^2=\text{const.} \tag{70}$$

and are more relevant to the example considered below.

Since the surface normal $\mathbf{n}$ for axisymmetric bodies has $n_\Phi=0, n_z=n_z(z)$, independent of Φ, it follows from (34) to (35) that for the pure translation $\alpha_z=\cos\vartheta_0+\imath\sin\vartheta_0\cos(\Phi-\Phi_\alpha)$, $\boldsymbol{\omega}\equiv 0$, the surface-normal velocity is

$$U_n=\boldsymbol{\alpha}\cdot\mathbf{n}=\Re\{\alpha_z\bar{n}_z\}=\cos\vartheta_0\cos(\sigma_W-\varphi)-\sin\vartheta_0\sin$$
$$(\sigma_W-\varphi)\cos(\Phi-\Phi_\alpha) \tag{71}$$

Hence, (14)–(16) admit single harmonics in Φ only for $\vartheta_0=0,\pi/2$, which corresponds, respectively, to translation parallel or perpendicular to the symmetry axis, with $m=0$, 1 in (67) and (70), respectively.

Conversely, for pure rotation, $\boldsymbol{\alpha}\equiv 0$, it is easy to show that

$$\begin{aligned} U_n&=\boldsymbol{n}\cdot(\boldsymbol{\omega}\times\mathbf{x}_{\mathrm{W}})=-\Im(\bar{n}_z z_{\mathrm{W}})\omega_\Phi\\ &=|\boldsymbol{\omega}_\perp|r_{\mathrm{W}}(\varphi)\sin\{\vartheta_{\mathrm{W}}(\varphi)+\sigma_{\mathrm{W}}(\varphi)-\varphi\}\sin(\Phi-\Phi_\omega)\end{aligned} \tag{72}$$

where the notation for components is that used in (60). Although the dependence on Φ that is similar to that of (71), the different dependence on φ generally rules out a simple harmonic solution for simultaneous rotation and translation, as is the case for the planar problem considered above and as will be made clear below.

Letting

$$\begin{aligned} &G_\varphi=R_{\mathrm{W}}t^3/h_{\mathrm{W}},\quad \Theta_{\mathrm{M}}=F_\varphi\cos m(\Phi-\Phi_0),\\ &\text{with}\quad \Theta=F_\varrho\Theta_{\mathrm{M}},\quad \Psi=S(\varrho)\Theta_{\mathrm{M}},\quad\text{and}\quad F_{\varrho\pm}=1\ \text{at}\ \varrho=1\end{aligned} \tag{73}$$

where Φ_0 is a constant, we can reduce (42) and (63) to the form

$$F''_\varphi+G_\varphi F'_\varphi+\left[\frac{h_{\mathrm{W}}M}{t^3}-m^2\frac{h_{\mathrm{W}}^2}{R_{\mathrm{W}}^2}\right]F_\varphi=0,\ \text{where}\ \Theta_{\mathrm{M}}=\frac{h_{\mathrm{W}}U_n}{M} \tag{74}$$

and M is defined by (44) with $F'_\pm\equiv F'_{\varrho\pm}$. Compatibility with (67) requires that $t(\varphi)$ satisfy

$$t^3=\frac{Mh_{\mathrm{W}}}{\lambda_\varphi+m^2(h_{\mathrm{W}}^2/R_{\mathrm{W}}^2-H_\varphi)} \tag{75}$$

where λ_ϕ is an appropriate characteristic value, and subscripts $\pm$ again refer to values at $\varrho=1\pm$.

To clarify these results, we consider the case of spheroids and the associated spheroidal harmonics.[27]

The cases of prolate and oblate spheroidal coordinates[27] Ch. X[**] are covered, respectively, by the substitutions

$$\{\hat{x},\hat{y}\}\rightarrow\begin{cases}\{\hat{Z},\hat{R}\} & (\text{prolate})\\ \{\hat{R},\hat{Z}\} & (\text{oblate})\end{cases} \tag{76}$$

in (45)–(47), with $h_{\mathrm{W}}=r_0|\sin(\varphi-\imath\chi_{\mathrm{W}})|$, $\chi_{\mathrm{W}}=-\ln\varrho_0$, according to (48) and (49). As the two geometries are related by a simple alteration of the map (45), we focus attention first on prolate spheroids and summarize key results for the oblate spheroids below.

Prolate spheroids

Then, the appropriate special case of (69) and (70) is

$$\begin{aligned} &\lambda_\varphi=n(n+1),\quad n=1,2,\ldots,\quad G_\varphi=\ln\sin\varphi,\\ &H_\varphi=\frac{1}{\sin^2\varphi},\ G_\varrho=\ln(\hat{\varrho}^2-1),\ H_\varrho=\frac{4}{(\hat{\varrho}^2-1)^2},\\ &R_{\mathrm{W}}(\varphi)=\frac{r_0}{2\varrho_0}(1-\varrho_0^2)\sin\varphi,\ H_{\mathrm{W}}=\frac{4\varrho_0^2}{(1-\varrho_0^2)^2}\end{aligned} \tag{77}$$

**cf. http://en.wikipedia.org/wiki/Prolate_spheroidal_coordinates, and http://en.wikipedia.org/wiki/Oblate_spheroidal_coordinates.

Table 2. Forces and Torques on Prolate Spheroids, with Parameters given by (47) and (85)

Motion (n, m)	$\mathbf{f}_\parallel$	$\mathbf{f}_\perp$	$\boldsymbol{\tau}_\perp$
Translation $\parallel(1,0)$	$-\frac{(1-\varrho_0^2)^3r_0^3\mathbb{N}^3}{3M\varrho_0^3}\boldsymbol{\alpha}_\parallel$	0	0
Translation $\perp(1,1)$	0	$-\frac{(1-\varrho_0^4)(1+\varrho_0^2)r_0^3\mathbb{N}^3}{3M\varrho_0^3}\boldsymbol{\alpha}_\perp$	0
Rotation $\perp(2,1)$	0	0	$-\frac{4(1-\varrho_0^2)r_0^5\mathbb{N}^3}{15M\varrho_0}\boldsymbol{\omega}_\perp$

and (75) takes on the form (43), with

$$t_0^3=\frac{F'_--k_{\mathrm{I}}F'_+}{n(n+1)+m^2H_{\mathrm{W}}} \tag{78}$$

Then, (64) and (65) reduce to

$$\begin{bmatrix}f_\perp\\ f_Z\end{bmatrix}=\frac{r_0^2(1-\varrho_0^2)\mathbb{N}^3}{2\pi\varrho_0^2}\int_{\varphi=0}^{\pi}\int_{\Phi=0}^{2\pi}\Theta_{\mathrm{M}}\begin{bmatrix}(1+\varrho_0^2)e^{\imath\Phi}\sin\varphi\\ (1-\varrho_0^2)\cos\varphi\end{bmatrix}\sin\varphi d\varphi d\Phi \tag{79}$$

$$\tau_\perp=-\frac{\imath r_0^3(1-\varrho_0^2)\mathbb{N}^3}{2\pi\varrho_0}\int_{\varphi=0}^{\pi}\int_{\Phi=0}^{2\pi}\Theta_{\mathrm{M}}e^{\imath\Phi}\sin 2\varphi\sin\varphi d\varphi d\Phi \tag{80}$$

The solutions F_ϱ, F_φ to (67) are both associated Legendre functions,[27] the latter given by multiples of the regular surface harmonics $P_n^m(\cos\varphi)$ and the former by $P_n^m(\lambda)$ or $Q_n^m(\lambda)$, inside and outside the surface W, respectively, with $\lambda=\cosh\chi$, where $\chi=\ln\hat{\varrho}$ is the variable appearing in (45)–(47).

The relations (71) and (72) now take on the simpler forms, for translation

$$\begin{aligned} h_{\mathrm{W}}U_n=&\frac{r_0}{2\varrho_0}[(1-\varrho_0^2)\alpha_Z\quad\cos\vartheta_0\cos\varphi\\ &+(1+\varrho_0^2)|\boldsymbol{\alpha}_\perp|\sin\vartheta_0\sin\varphi\ \cos(\Phi-\Phi_\alpha)]\end{aligned} \tag{81}$$

and, for rotation

$$h_{\mathrm{W}}U_n=-\frac{|\boldsymbol{\omega}_\perp|r_0^2}{2}\sin 2\varphi\ \sin(\Phi-\Phi_\omega) \tag{82}$$

with Θ_{W} given by the second equation of 74. Owing to axial symmetry, we may without loss of generality set Φ_α and Φ_ω equal to zero.

In view of the well-known expressions for associated Legendre functions and their derivatives,[27–29] it is evident that (81) involves two distinct surface harmonics, with $n=1$, $m=0$, and $P_1^0\equiv P_1=\cos\varphi$, and with $n=1$, $m=1$, and $P_1^1=-\sin\varphi$, respectively, whereas (82) involves a single harmonic with $n=2$, $m=1$, and $P_2^1=-3\sin 2\varphi/2$. We note that the doubly periodic form for $n=2$ involves two melting and two regelation zones, as was the case with rotation of elliptic cylinders. Then, for each pair of integers n, m we have a distinct harmonic motion, with

$$F_\varrho=\begin{cases}P_n^m(\cosh\chi)/P_n^m(\cosh\chi_{\mathrm{W}}), & \text{for}\ \varrho\le 1,\\ & \text{where}\ \chi=\ln(\varrho/\varrho_0)\\ Q_n^m(\cosh\chi)/Q_n^m(\cosh\chi_{\mathrm{W}}) & \text{for}\ \varrho\ge 1,\end{cases} \tag{83}$$

where t_0 is given by (78) and the Legendre functions are given for real arguments x by

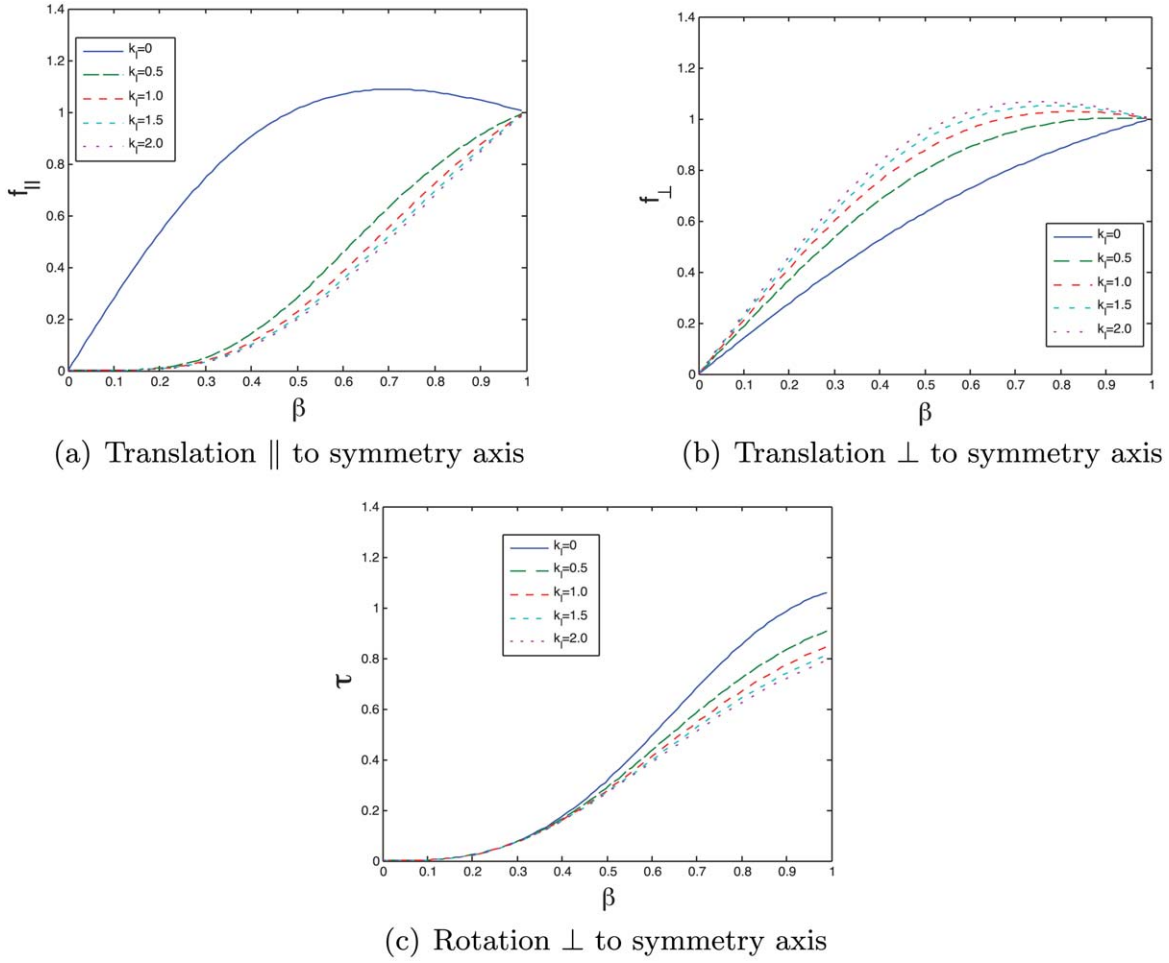

Figure 2. Force and torque on prolate spheroids as functions of axis ratio β, given by Table 2 and (89), with forces in (a) and (b) normalized by force on sphere (β=1), and with torques in (c) normalized by torque on elliptic cylinder having same β.

(a) Translation ‖ to symmetry axis. (b) Translation ⊥ to symmetry axis. (c) Rotation ⊥ to symmetry axis. [Color figure can be viewed in the online issue, which is available at wileyonlinelibrary.com.]

$$P_n^m(x)=(x^2-1)^{m/2}\left(\frac{d}{dx}\right)^m P_n(x)=\frac{1}{2^n n!}(x^2-1)^{m/2}\left(\frac{d}{dx}\right)^{m+n}(x^2-1)^n$$

and

$$Q_n^m(x)=(x^2-1)^{m/2}\left(\frac{d}{dx}\right)^m Q_n(x),\quad \text{for}\quad m,n=0,1,2,\ldots \tag{84}$$

on taking $z=x$ in Eqs. 8.4.1-6–8.6.6-7, and 8.6.18 of Ref. 28.

Although all the Legendre functions encountered here can be expressed in terms of elementary functions, Eq. 8.2.5 of Ref. 28 plus Eqs. 14.3.7 and 14.3.18 of Ref. 29, combined with MATLAB® computation of hypergeometric functions, were found useful for numerics.

Hence, the final equation of 74, together with (83), and standard formulae for Legendre functions,[28] gives

$$M=\frac{s}{c^2-1}\left\{(n+1)(k_1-1)c+(n-m+1)\left[\frac{P_{n+1}^m(c)}{P_n^m(c)}-k_1\frac{Q_{n+1}^m(c)}{Q_n^m(c)}\right]\right\},$$

$$\text{for } n=1,2,\ m=0,1,\ \text{with}\quad c=\cosh\chi_W=\frac{1+\varrho_0^2}{2\varrho_0},\ s=\sinh\chi_W=\frac{1-\varrho_0^2}{2\varrho_0} \tag{85}$$

where M has been obtained from $F'_{\pm}$ by means of (44).

From these results and (79), (80), it is a simple matter to derive the nondimensional forces and torques shown as space vectors in Table 2, where subscripts $\|,\perp$ refer to vector projections parallel and perpendicular to the symmetry axis, respectively, and where, with proper scaling, $\boldsymbol{\alpha}$ and $\boldsymbol{\omega}$ represent unit vectors.

The factors M are given as functions of ϱ_0 by well-known formulae for the Legendre functions.[28,29] Also, we recall once again that the parameters r_0,ϱ_0 are given in terms of the axis ratio β by (47).

Oblate spheroids

Summarized here are the major changes of the above results for prolate spheroids. In particular, replacing $\hat{z}(\hat{\zeta})$ in (45) by $\check{z}=\imath\hat{z}(\zeta)$ requires the following modifications. First, (77) is replaced by

$$G_\varphi=\ln\cos\varphi,\quad H_\varphi=\frac{1}{\cos^2\varphi},\quad G_\varrho=\ln(\hat{\varrho}^2+1),$$

$$H_\varrho=\frac{4}{(\hat{\varrho}^2+1)^2},\quad R_W(\varphi)=\frac{r_0}{2\varrho_0}(1+\varrho_0^2)\sin\varphi,\quad H_W=\frac{4\varrho_0^2}{(1+\varrho_0^2)^2} \tag{86}$$

whereas (79), (80) become

$$\begin{bmatrix} f_\perp \\ f_Z \end{bmatrix} = \frac{r_0^2(1+\varrho_0^2)\mathbb{N}^3}{2\pi\varrho_0^2}\int_{\varphi=0}^{\pi}\int_{\Phi=0}^{2\pi} \Theta_M \begin{bmatrix} (1+\varrho_0^2)e^{\imath\Phi}\sin\varphi \\ (1-\varrho_0^2)\cos\varphi \end{bmatrix} \cos\varphi d\varphi d\Phi \tag{87}$$

$$\tau_\perp = \frac{\imath r_0^3(1+\varrho_0^2)\mathbb{N}^3}{2\pi\varrho_0}\int_{\varphi=0}^{\pi}\int_{\Phi=0}^{2\pi} \Theta_M e^{\imath\Phi}\sin 2\varphi\cos\varphi d\varphi d\Phi \tag{88}$$

Hence, the coefficients of $-\boldsymbol{\alpha}_\parallel$, $-\boldsymbol{\alpha}_\perp$, and $-\boldsymbol{\omega}_\perp$ in Table 2 are replaced, respectively, by

$$\frac{(1-\varrho_0^4)(1+\varrho_0^2)r_0^3\mathbb{N}^3}{3M\varrho_0^3},\ \frac{(1+\varrho_0^2)^3 r_0^3\mathbb{N}^3}{3M\varrho_0^3},\ \text{and}\ \frac{4(1+\varrho_0^2)r_0^5\mathbb{N}^3}{15M\varrho_0} \tag{89}$$

As the harmonics associated with (86) are $P_n^m(\cos\varphi)$ and $P_n^m(\imath\sinh\chi)$ or $Q_n^m(\imath\sinh\chi)$,[27] the relations (83)–(85) carry through, with χ and χ_W replaced everywhere by $\chi+\imath\frac{\pi}{2}$ and $\chi_W+\imath\frac{\pi}{2}$, respectively.

It is easy to verify that the forces given in Table 2 and (89) reduce to (58) when the spheroid becomes spherical. Otherwise, these results involve a shape dependence made evident by Figure 2, which presents calculations of various drag coefficients for prolate spheroids as functions of aspect ratio β, with k_I, the ratio of ice to body conductivity, as parameter. The drag forces are scaled by the values for the sphere, $\beta=1$, while torque is scaled by the torque on unit length of an elliptic cylinder having the same β.

Owing the logarithmic singularity of the Legendre function $Q_1(c)$ in (85) at $\beta=0$, where $c=1$, the parallel drag coefficients in Figure 2a exhibits singular behavior at $k_I=0$, reflecting a physical singularity for bodies B with infinite conductivity. This is clearly a 3-D effect, as no such singularity arises in the 2-D case. Once again, the shape dependence is not captured by Nye's formula[7] Eq. 15 for Case (1 A), $\epsilon=0, k_I=0$.

Conclusions

The foregoing generalization of the work of Nye provides analytic results for drag force and torque on solid elliptic cylinders and spheroids moving through ice under the action of pressure melting, regelation, and flow in a lubricating water layer. The analysis is based on the assumption of negligible thermal resistance of the water layer which allows for special harmonic solutions for various uncoupled translations and rotations of elliptical cylinders and spheroids. The results show a dependence on body shape not captured by the certain formulae proposed by Nye, and they indicate a concomitant variation of the water-layer thickness t as the 1/3-power of the surface-normal metrical coefficient. There is an interesting question as to whether this variation of t may remain valid for more complicated motions, a question that might possibly be settled by numerical solution of the general equations proposed earlier.

The present analysis suggests simple experiments involving slow steady rotation of solid bodies such as elliptic cylinders in a stationary block of ice, as an alternative to unsteady experiments involving translation of a wire or other solid body. Such experiments could provide easier experimental observation and serve to elucidate certain discrepancies between the Nye theory and experiment, perhaps leading to improvements in the theory such as those proposed by Drake and Shreve.[12]

Although the present analysis is devoted to analytical solutions for the case of thermally thin melt layers around simple body shapes, it by no means excludes experiments on more complex geometries. In that regard, it is worth recalling that, despite its ubiquity and unique molecular properties, water is by no means the only candidate for the kind of experiment considered above. As indicated by the Clapeyron equation, the pressure-melting will generally occur in any substance with negative volume of fusion, a subject of considerable and sustained theoretical interest in its own right.[30–34] Although the extreme conditions of melting, or the optical opacity of solid and liquid, would rule out experiments of the type appropriate to the water–ice system, there remain certain interesting possibilities. A cursory review of the literature turns up a wide variety of materials exhibiting contraction on melting, including lanthanide and actinide metals[35]; germanium[36,37]; gallium and bismuth[38,39]; alkali halides[31]; some alkali nitrates[40]; certain macromolecular compounds[33]; and possibly, diamond.[41]

Acknowledgments

Many years ago an undergraduate at the University of Illinois UIUC listened, awe-struck, to an elegant seminar on the thermodynamics of fluid flow presented by a rising academic star from the University of Wisconsin and alumnus of the U of I. The erstwhile undergraduate offers this article as modest tribute to the star who has continued to shine so brightly over the intervening years.

Literature Cited

1. Thomson J. Theoretical considerations on the effect of pressure in lowering the freezing point of water. *Trans Roy Soc Edin.* 1848; 16(5):575–580.
2. Thomson W. XII. The effect of pressure in lowering the freezing-point of water experimentally demonstrated. *Philos Mag Ser 3.* 1850;37(248):123–127.
3. Thomson J. On crystallization and liquefaction, as influenced by stresses tending to change of form in the crystals. *Proc R Soc London.* 1860;11:472–481.
4. Faraday M. *Experimental Researches in Chemistry and Physics.* London: Taylor & Francis, 1859.
5. Faraday M. Note on regelation. *Proc R Soc London.* 1859;10:440–450.
6. Ornstein LS. Motion of a wire through a lump of ice. *Proc Kon Ned Akad Wet.* 1906;14:629–635. (in Dutch).
7. Nye JF. Theory of regelation. *Philos Mag.* 1967;16:1249–1266.
8. Frank FC. Regelation: a supplementary note. *Philos Mag.* 1967; 16(144):1267–1274.
9. Mullins WW, Sekerka RF. Stability of a planar interface during solidification of a dilute binary alloy. *J Appl Phys.* 1964;35(2):444–451.
10. Davis SH. *Theory of Solidification.* Cambridge, New York: Cambridge University Press, 2001.
11. Worster MG. Convection in mushy layers. *Annu Rev Fluid Mech.* 1997;29(1):91–122.
12. Drake LD, Shreve RL. Pressure melting and regelation of ice by round wires. *Proc R Soc London A.* 1973;332(1588):51–83.
13. Taylor GI. Cavitation of a viscous fluid in narrow passages. *J Fluid Mech.* 1963;16(4):595–619.
14. Nye JF. A calculation on the sliding of ice over a wavy surface using a Newtonian viscous approximation. *Proc R Soc London A.* 1969;311(1506):445–467.
15. Nye JF. Glacier sliding without cavitation in a linear viscous approximation. *Proc R Soc London A.* 1970;315(1522):381–403.
16. Evans DCB, Nye JF, Cheeseman KJ. The kinetic friction of ice. *Proc R Soc London A.* 1976;347(1651):493–512.
17. Colbeck SC, Najarian L, Smith HB. Sliding temperatures of ice skates. *Am J Phys.* 1997;65(6):488–492.
18. Dash JG, Fu H, Wettlaufer JS. The premelting of ice and its environmental consequences. *Rep Prog Phys.* 1995;58(1):115–167.

19. Rosenberg R. Why is ice slippery? *Phys Today*. 2005;58(12):50–55.
20. Wettlaufer JS, Worster MG. Premelting dynamics. *Annu Rev Fluid Mech*. 2006;38(1):427–452.
21. Hynninen T, Heinonen V, Dias C, Kartunnen M, Foster A, Ala-Nissila T. Cutting ice: nanowire regelation. *Phys Rev Lett*. 2010;105(8): 086102.
22. Pinkus O, Sternlicht B. *Theory of Hydrodynamic Lubrication*. McGraw-Hill: New York, 1961.
23. Tyvand P, Bejan A. The pressure melting of ice due to an embedded cylinder. *J Heat Trans (ASME)*. 1992;114(2):532–535.
24. Lamb H. *Hydrodynamics*. Cambridge, UK: Cambridge University Press, 1916.
25. Miloh T, Benveniste Y. On the effective conductivity of composites with ellipsoidal inhomogeneities and highly conducting interfaces. *Proc R Soc A*. 1999;455(1987):2687–2706.
26. Moon P, Spencer DE. Recent investigations of the separation of Laplace's equation. *Proc Am Math Soc*. 1953;4(2):302–307.
27. Hobson EW. *The Theory of Spherical and Ellipsoidal Harmonics*. Cambridge, UK: Cambridge University Press, 1931.
28. Abramowitz M, Stegun I. *Handbook of Mathematical Functions, Volume 55 of Applied Mathematics Series*. New York: U.S. National Bureau of Standards, 1965.
29. Olver F, Lozier D, Bolsvert R, Clark C, editors. *NIST Handbook of Mathematical Functions*. U.S. National Institute of Standards and Technology & Cambridge University Press: New York, 2010. Available at http://dlmf.nist.gov/14.3. Last accessed on May 6, 2013.
30. Stishov SM. The thermodynamics of melting of simple substances. *Sov Phys Usp*. 1975;17(5):625.
31. Tallon JL. The entropy change on melting of simple substances. *Phys Lett A*. 1980;76(2):139–142.
32. Stillinger FH, Debenedetti PG. Phase transitions, Kauzmann curves, and inverse melting. *Biophys Chem*. 2003;105(23):211–220.
33. Feeney MR, Debenedetti PG, Stillinger FH. A statistical mechanical model for inverse melting. *J Chem Phys*. 2003;119(8):4582–4591.
34. Lu HM, Jiang Q. Melting volume change of different crystalline lattices. *Phys Stat Solidi B*. 2004;241(11):2472–2476.
35. Wittenberg LJ, DeWitt R. Volume contraction during melting; emphasis on lanthanide and actinide metals. *J Chem Phys*. 1972; 56(9):4526–4533.
36. Sangster RC, Carman JN. Contraction of germanium on melting. *J Chem Phys*. 1955;23(1):206–207.
37. Vaidya SN, Akella J, Kennedy GC. Melting of germanium to 65 kbar. *J Phys Chem Solids*. 1969;30(6):1411–1416.
38. Cusack N, Kendall P. A note on the viscosity and resistivity of liquid gallium. *Proc Phys Soc*. 1960;75(2):309.
39. Singh A, Tsai AP. Melting behaviour of lead and bismuth nanoparticles in quasicrystalline matrix—the role of interfaces. *Sadhana*. 2003;28(1–2):63–80.
40. Owens BB. Melting properties of the alkali nitrates to 10 000 atmospheres. *J Chem Phys*. 1965;42(7):2259–2262.
41. Brygoo S, Henry E, Loubeyre P, Eggert J, Koenig M, Loupias B, Benuzzi-Mounaix A, Rabec Le Gloahec M. Laser-shock compression of diamond and evidence of a negative-slope melting curve. *Nat Mater*. 2007;6(4):274–277.

Manuscript received Aug. 31, 2013, and revision received Nov. 29, 2013.